DE GRUYTER

Biomed. Eng.-Biomed. Tech. 2022; 67(1): 33–42

Michael Schweigmann, Frank Kirchhoff and Klaus P. Koch*

Comparative study of platinum electroplating to improve micro gold electrode arrays with LCP laminate

Abstract: Decoding the cellular network interaction of neurons and glial cells are important in the development of new therapies for diseases of the central nervous system (CNS). Electrophysiological *in vivo* studies in mice will help to understand the highly complex network. In this paper, the optimization of epidural liquid crystal polymer (LCP) electrodes for different platinum electroplating parameters are presented and compared. Constant current and pulsed current electroplating varied in strength and duration was used to decrease the electrode impedance and to increase the charge storage capacity (CSC_C). In best cases, both methods generated similar results with an impedance reduction of about 99%. However, electroplating with pulsed currents was less parameter-dependent than the electroplating with constant current. The use of ultrasound was essential to generate platinum coatings without plating defects. Electrode model parameters extracted from the electrode impedance reflected the increase in surface porosity due to the electroplating processes.

Keywords: charge storage capacity (CSC_C); electrode impedance; electrode model; electroplating; platinum; pulsed current; ultrasound.

Introduction

Many different diseases or injuries of the central nervous system (CNS) have a great disabling impact on everyday life. A better understanding of the cellular signaling and network interaction might help to develop better therapies. With murine *in vivo* studies the CNS can be investigated in many different pathological models, such as epilepsy [1] or traumatic brain injury [2].

Electrophysiology is one approach to record or to induce cell activity in living animals. Thus, cost-effective electrodes made from a liquid crystal polymer (LCP) with two different gold electrode sites were developed (Figure 1). Electroplated nanoporous platinum on the top of the electrode sites could improve the effective surface area and thereby, the electrodes' electrochemical properties. Changing the plating parameters such as the electrode overpotential and the structure of the base substrate, varies the structure of platinum coating [3]. In order to find the possible best electrochemical improvement for these type of LCP electrodes, different electroplating processes were tested. Plating with pulsed currents to periodically change the electrode potential were compared with constant currents, both varied in amplitude and in electroplating time. In addition, the influence of ultrasound application during the electroplating process was investigated, because some improvements were reported previously [4, 5]. With cyclic voltammetry and impedance spectroscopy common techniques were used to characterize the electrochemical properties of the electrode [6]. Cyclic voltammetry characterized the electrochemical reactions at the electrode surface and therewith the charge transfer ability [6, 7]. Electrochemical impedance spectroscopy described the small signal frequency behavior of the electrodes, which might be important for electrical stimulation [8] or for electrical recording [9].

Materials and methods

LCP electrodes

The selected LCP technology [10] consisted of three polymer layers, each 25 µm thick. The outer layers served as base and top insulation, which were connected with the inner adhesive layer. The electrical structure was formed with two layers of gold. An inner gold layer served as the interconnection plane and, the outer layer formed the electrode sides and solder pads. Both gold layers were connected by gold vias, which were produced by a galvanic process. Electrode

*Corresponding author: Klaus P. Koch, Department of Electrical Engineering, Trier University of Applied Sciences, Trier, Germany, Phone: +49 651 8103 514, E-mail: koch@hochschule-trier.de
Michael Schweigmann, Department of Electrical Engineering, Trier University of Applied Sciences, Trier, Germany; and Department of Molecular Physiology, Center for Integrative Physiology and Molecular Medicine, University of the Saarland, Homburg, Germany, E-mail: michael.schweigmann@uks.eu
Frank Kirchhoff, Department of Molecular Physiology, Center for Integrative Physiology and Molecular Medicine, University of the Saarland, Homburg, Germany, E-mail: frank.kirchhoff@uks.eu
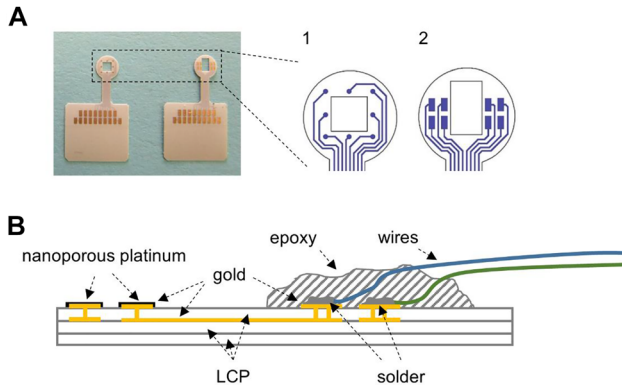
Figure 1: Overview of the liquid crystal polymer (LCP) electrodes. (A) Design of the surface electrode array consisting of the round-shaped electrode head, the connector area and a small catwalk. (1) Eight channel electrode with round-shaped electrode sites of 150 μm in diameter. (2) Eight channel electrode with rectangular-shaped electrode sites of 400 μm × 200 μm. (B) Cross section of the LCP technology and assembling of the electroplating probes.

arrays with round-shaped electrode sites with a diameter of 150 μm or rectangular-shaped electrodes with a size of 400 μm × 200 μm were designed (Figure 1A). To prepare the electroplating probes (Figure 1B), individual small wires (108.301.12.36/PFA, Ø 0.0123 mm², Rotronik-Kabel) were soldered on the terminal pads with a low-temperature solder paste (CR11, EDSYN GmbH Europe). The connections were covered with epoxy resin (TC-EP05-24, TOOLCRAFT) for mechanical fixation and electrical insulation.

Electroplating set-up

An electroplating system was built up including a LabView control software, a digital-to-analog converter (NI USB-6003, National Instruments) and a voltage-controlled stimulator (ISO-STIM01D, NPI electronic GmbH). A large mesh electrode (platinized titanium, Jentner Plating Technology GmbH) acted as a counter electrode. The electroplating solution was made of 5 g hexachloroplatinic acid (H_2PtCl_6, Sigma–Aldrich Co. LLC) dissolved in 375 mL distilled water [11, 12]. Enabling ultrasound application during the electroplating process, 80 mL of the platinum solution within a beaker was placed in a basin equipped with an ultrasound module (Emmi®-12HC, EMAG AG) and filled with tap water.

Electroplating parameters

The round-shaped electrodes were treated with constant currents (current densities: 0.1–0.4 kA/m², step 0.1 kA/m²) and with pulsed currents (current densities: 0.2 kA/m², 0.3 kA/m², 0.4 kA/m²) and the rectangular electrodes with pulsed currents (current densities: 0.2 kA/m², 0.3 kA/m², 0.4 kA/m²). Pulse times of 1 s, 0.667 s, and 0.5 s and a pause time of 1 s were selected to use the same amount of charge

transfer in each process and to achieve stationary electrode potentials during current pulse application. In constant current application plating times between 30 s and 90 s, in pulsed current application 60 pulses, 90 pulses, and 120 pulses were used. The impact of ultrasound power (settings: 50%, 100%) was investigated by variation of the intensity for electroplating with pulsed current of the round-shaped electrodes. For the electroplating with constant current and for the rectangular-shaped electrodes, the ultrasound module was set to 50%.

Electrochemical characterization

Electrochemical characterization was performed with a commercially available measuring system (Interface 1000, Gamry Instruments), 0.9% saline solution, a large stainless steel counter electrode (220 mm²), and a silver/silver chloride reference electrode (RE-1B, ALS Co. Ltd.). A sequence of cyclic voltammetry (voltage limits: from −0.5 V to +0.7 V against reference electrode potentials, scan speed: 1 V/s), observation of the open circuit potential (OCP) (time: 300 s) and impedance spectroscopy (frequency range: from 1 Hz to 100 kHz; amplitude 50 mV) was used before and after electroplating. The voltage range of the CV was chosen to stay safely within the water window of platinum in saline (from −0.6 V to 0.8 V vs. Ag/AgCl [6]) and for reasons of laboratory internal comparison. With the analysis software Gamry Echem Analyst V6.20 (Gamry Instruments) the cathodic charge storage capacity (CSC_C) [6], the electrode model parameters, and the magnitude of the electrode impedance at 10 Hz were determined. The value at 10 Hz was selected due to the impedance characteristics of these LCP electrodes. Only the solution resistances were visible at the often used frequency of 1 kHz (Figure 2A). The common model for metal electrodes with a constant phase element (CPE) parallel to a diffusion resistance (R_F) and a solution resistance in series (R_S) was selected [13].

Peel and pulse test

To test the stability of the platinum coatings produced with pulsed currents (0.2 kA/m² and 0.3 kA/m²; with and without ultrasound application), a peel test [14, 15] was performed using the Scotch® 508 adhesive tape. The electrode sites and tape were optical inspected with a microscope camera (a2A1920-160ucPRO, Basler AG). In addition, after estimation of the charge injection capacity (CIC) [16, 17] for platinum coated electrodes (pulsed current, 0.3 kA/m², 90 pulses, ultrasound power 50%), a durability test with 300,000 biphasic stimulation pulses was done. With respect to the estimated CIC, two different current pulses with an amplitude of ±530 μA at a pulse width of 200 μs and an amplitude of ±400 μA at a pulse width of 500 μs were applied with a single channel stimulator (ISO-STIM 01D; NPI electronic). The electrode potential against a silver/silver chloride reference electrode (RE-1B, ALS Co. Ltd.) was measured with a standard oscilloscope (Tektronix, MSO2024). Electrode impedances were measured prior and after the pulse test. For the peel and the pulse test, the electrode with the rectangular-shaped sites was chosen because it was used for *in vivo* stimulation studies in mice [18].
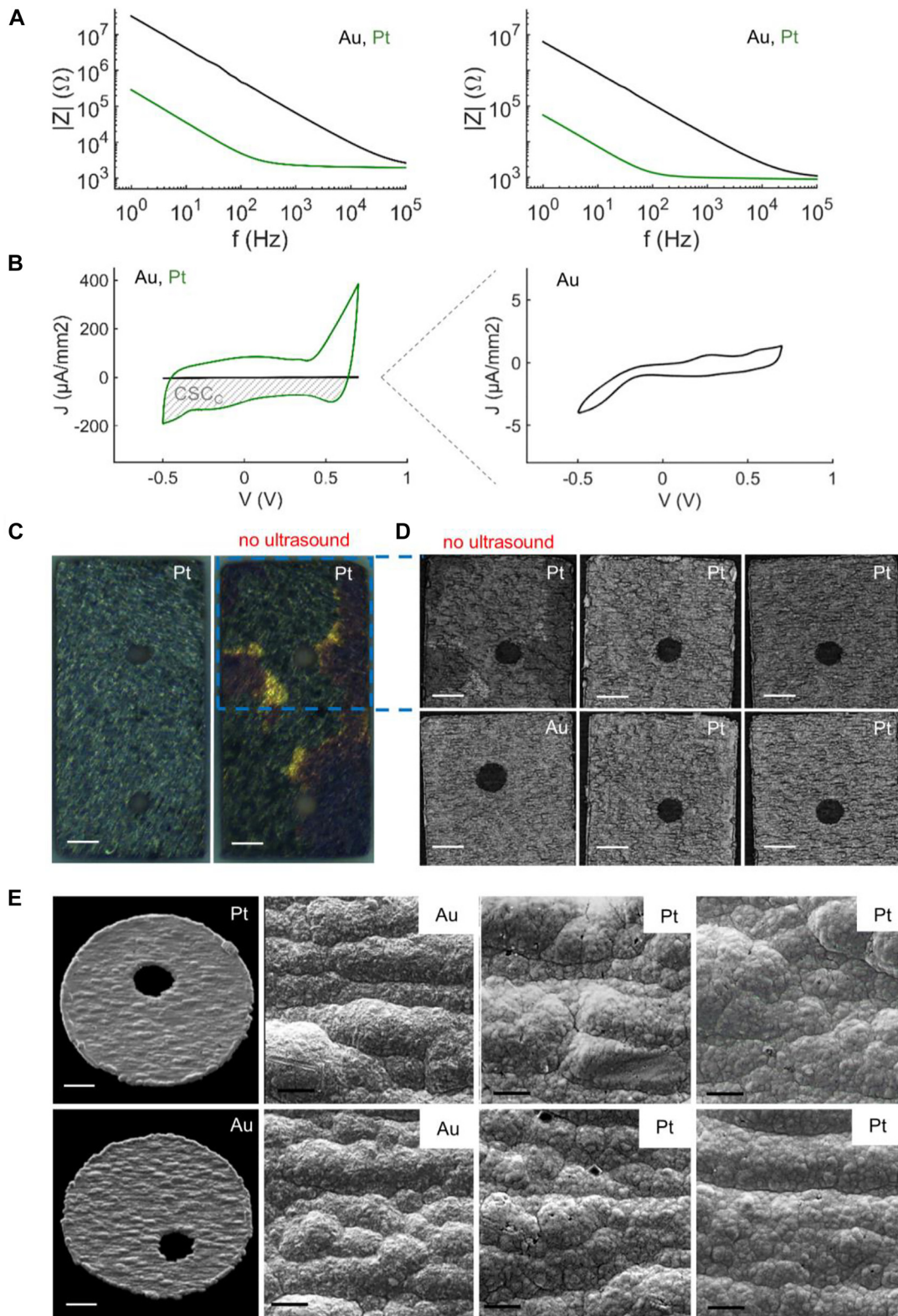
Figure 2: Examples of electroplating results.
(A) Magnitudes of impedance (|Z|) for round-shaped electrodes (left) and rectangular-shaped electrodes (right) prior and after electroplating (left: constant current 0.2 kA/m2, 75 s; right: pulsed current, 0.3 kA/m^2, 90 pulses). (B) Comparison of cyclic voltammograms of a non-coated and coated rectangular-shaped electrode site (pulsed current, 0.3 kA/m^2, 90 pulses; J, current density; V, electrode voltage). (C) Microscopic

Results

Platinum electroplating improved electrochemical characteristics and application of ultrasound prevented coating defects

The platinum coatings of the gold electrodes reduced the electrode impedance and increased the CSC_C in all galvanic studies (examples in Figure 2A, B; see Supplementary Material for all measurements). During the electroplating processes with current densities above or equal to 0.3 kA/m^2, gas bubbles were clearly visible on the surface of the electrode sites. The bubbles generated by water electrolysis isolated the surface and incomplete and inhomogeneous platinum coating appeared (Figure 2C; images taken with microscope M205 C (Leica Microsystems)). In addition to the defects visible immediately after the electroplating process, the size and number of the defects was increased after applying the usually non-destructive electrochemical characterization. With the use of ultrasound, the bubbles at the electrode surface could be removed and the platinum electroplating took place over the entire electrode surface. The defects in the platinum coating could be also observed with the surface measuring system Confovis TOOLinspect (Confovis GmbH) in the absence of ultrasound (Figure 2D). Moreover, the optical images revealed the base rough structure of the gold electrode sites that altered with the platinum coating. This could be confirmed with scanning electron microscopy (SEM, XL30 ESEM FEG [FEI/Philips]). The images displayed the rough surface from the gold electrode and a ball like structure from the platinum coating (Figure 2E).

Electroplating with constant current was highly parameter-dependent and best at a current density of 0.2 kA/m^2

The impedance magnitude at a frequency of 10 Hz ranged (over all values) from approximately 30 kΩ to 400 kΩ (Figure 3A). The values showed a high dependency on the electroplating parameters and were highest (mean values around 300 kΩ) with a current density of 0.1 kA/m^2. A half of this electrode impedance could be achieved with 0.3 kA/m^2 and 0.4 kA/m^2 for the selected plating times. In addition, the results for the two highest current densities did not show a significant difference (mean values between 130 kΩ and 180 kΩ). The lowest impedance with a mean value of approximately 40 kΩ could be achieved with a current density of 0.2 kA/m^2. The impedance magnitude decreased gradually with increasing electroplating time until a plating time of 75 s was reached. Thereafter, an increase in the impedance magnitude was visible, indicating that the highest surface roughness had already been achieved. Compared to the gold electrodes (| $Z(f = 10 \text{ Hz})$| = 3.3–7.2 MΩ), the impedance reduction was always over 90%. In the best case, the impedances were reduced to a value of about 1% from the original values.

With the electroplating processes, cathodic CSC_Cs in the range of approx. 1,500 µC/cm^2 to 10,000 µC/cm^2 could be achieved (Figure 3A). The trend of all values was in line with the electrode impedance magnitude, showing the best result at a current density of 0.2 kA/m^2 and an electroplating time of 75 s. The mean values of the OCP were mostly in the range of 0.41–0.48 V with a variation of approximately 50 mV within one electroplating condition. Only the OCP values of the third process (0.2 kA/m^2, 30 s) were around 0.1 V. This large difference indicated incomplete platinum coatings.

Pulsed current electroplating were less parameter-dependent as constant current electroplating

Electroplating with pulsed currents was performed at three different current densities (0.2 kA/m^2, 0.3 kA/m^2, 0.4 kA/m^2) and three different number of current pulses (60 pulses, 90 pulses, 120 pulses). In addition, the influence of the settable ultrasound power of the basin (50% or 100%) were tested with the round-shaped electrodes.

images (M205 C [Leica Microsystems]) of electrodes (scale bar: 40 µm) after electroplating (0.3 kA/m^2) with (left) and without (right) ultrasound. (D) Optical images (scale bar: 40 µm) taken with a surface measuring system TOOLinspect (Confovis GmbH). Upper row from left to right: structures of (1) constant current electroplating 0.3 kA/m^2; 60 s, no ultrasound; (2) constant current electroplating 0.2 kA/m^2, 75 s, ultrasound 50%; (3) constant current electroplating 0.3 kA/m^2, 60 s, ultrasound 50%; lower row from left to right: structures of (1) gold electrode; (2) pulsed current electroplating 0.2 kA/m^2; 90 pulses, ultrasound 50%; (3) pulsed current electroplating 0.3 kA/m^2; 90 pulses, ultrasound 50%. (E) SEM images (XL 30 ESEM FEG; FEI/PHILIPS) showing the round-shaped electrode (scale bar: 25 µm) and surface structures (scale bar: 2 µm) of the gold and platinum sites (all pictures from different electrode sites). Zoom-Views: Left: Au; Middle: Pt, constant current electroplating 0.2 kA/m^2, 75 s; ultrasound 50%. Right: Pt, pulsed current electroplating 0.3 kA/m^2, 90 pulses, ultrasound 50%.
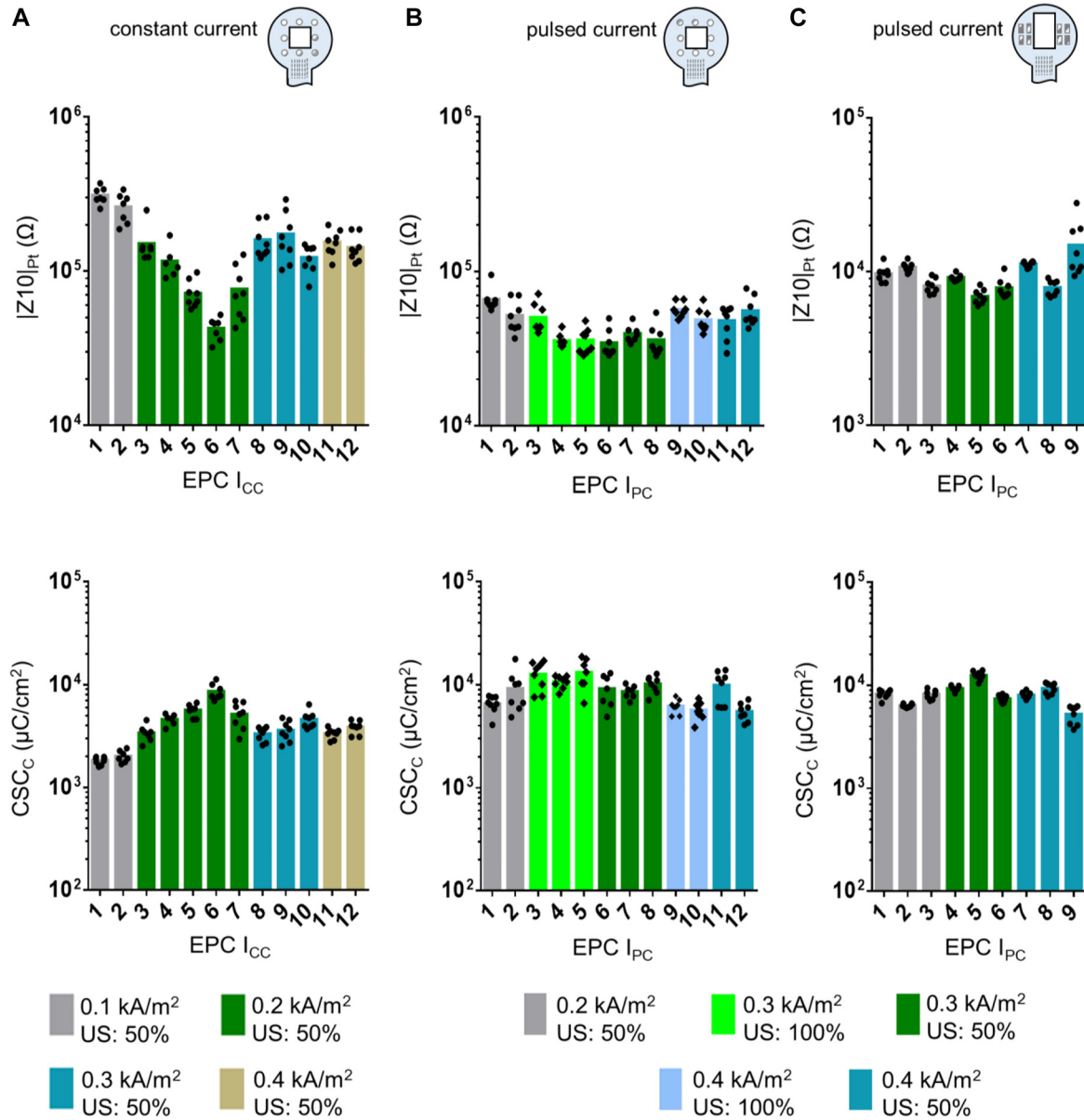
Figure 3: Electroplating results for platinized electrode sites.

Top row: magnitude of impedance at 10 Hz ($|Z10|_{Pt}$). Bottom row: charge storage capacity (CSC_C). (A) Round-shaped electrodes and constant current (I_{CC}). 1: 60 s, 2: 75 s, 3: 30 s, 4: 45 s, 5: 60 s, 6: 75 s, 7: 90 s, 8: 30 s, 9: 60 s, 10: 90 s, 11: 30 s, 12: 60 s. (B) Round-shaped electrodes and pulsed current (I_{PC}). 1: 60 pulses, 2: 90 pulses, 3: 60 pulses, 4: 90 pulses, 5: 120 pulses, 6: 60 pulses, 7: 90 pulses, 8: 120 pulses, 9: 60 pulses, 10: 90 pulses, 11: 60 pulses, 12: 90 pulses. (C) Rectangular-shaped electrodes and pulsed current. 1: 60 pulses, 2: 90 pulses, 3: 120 pulses, 4: 60 pulses, 5: 90 pulses, 6: 120 pulses, 7: 60 pulses, 8: 90 pulses, 9: 120 pulses. Y-axis of $|Z10|_{Pt}$ is in another scale as for the round-shaped electrodes.

Round-shaped electrodes

For the round-shaped electrodes, the magnitude of the electrode impedance at the frequency of 10 Hz were lower than 100 kΩ for all pulsed current electroplating processes (Figure 3B). Compared to the impedance magnitudes of the gold electrode, these values were in the

range of 1–4% from the original values. Across the different electroplating current densities, the electroplating processes with 0.2 kA/m² resulted in the same impedance range than the electroplating processes with 0.4 kA/m². The impedance magnitudes generated with a plating current of 0.3 kA/m² were approximately 20% lower than in the other conditions. The number of applied pulses had

only an effect on the electrodes' impedance, when low currents or small number of electroplating pulses were used. No difference between 50% or 100% US power could be clearly identified. Compared to the electroplating with constant currents, the impedances after both electroplating methods were in the best cases close together. In line with the results of the impedance magnitudes, the achieved CSC_C were best for the electroplating with a current density of 0.3 kA/m^2 ranging from 9,200 μC/cm^2 to 12,700 μC/cm^2. With that, the CSC_C was also in the same range as in the constant current electroplating and there was no indication that the ultrasound power had an impact on the result. The OCP mean values were within 0.42–0.49 V indicating complete platinum coatings.

Rectangular-shaped electrodes

The measured impedance magnitudes at 10 Hz of the rectangular-shaped electrodes were in the range from 6 kΩ to 28 kΩ (Figure 3C). The best results were achieved at 0.2 kA/m^2 with 120 pulses and 0.3 kA/m^2 with 90 pulses. The electrode impedances were worst using current densities of 0.4 kA/m^2. The reduced impedances were within 1–5% compared to the impedance of the gold sites ($|Z(f = 10$ Hz$)| = 0.5$–1.1 MΩ). Taking the geometric surface area into consideration, an 'area impedance' could be calculated by impedance magnitude multiplied with geometric surface area. Over all measures, for the rectangular electrodes, values from 0.48 kΩmm^2 (6 kΩ) to 2.24 kΩmm^2 (20 kΩ), and for the round-shaped electrodes coated with pulsed currents values from 0.54 kΩmm^2 (30 kΩ) to 1.8 kΩmm2 (100 kΩ) were estimated. With a current density of 0.3 kA/m^2 and 90 current pulses the values were 0.54–0.9 kΩmm^2 for the round-shaped electrodes and from 0.48 kΩmm^2 to 0.68 kAmm^2 for the rectangular-shaped electrodes. This indicated that the electroplating process produced comparably surface porosities for both types of electrodes. The CSC_C were highest for 0.3 kA/m^2 and 60 pulses with values around 12.000 μC/mm^2. Considering the higher variation of the CSC_C of the round-shaped electrodes, the values of the rectangular-shaped electrodes were also similar to the previous one. The mean OCP ranged from 0.39 V to 0.49 V.

Electrode model parameters reflect the increase in surface porosity

The extraction of the model parameters (CPE, R_S, R_F) was done for all measurements of platinum electrodes. Owing to the size of the electrode sites and the measurement

frequency range, R_F could not be reliably determined (values from 1 MΩ to 1 TΩ). For analyzation of the model parameters, R_S and the angle factor (α) of the CPE were set in relation to the admittance value (Y_0) of the CPE (Figure 4).

R_S for the round-shaped electrodes after both electroplating methods was in the range of 2 kΩ ± 300 Ω, indicating some tolerances in the electroplating solution (platinum ion concentration, solution temperature) and in the measurements (variation in room temperature) as well as manufacturing tolerances of the electrode sites (Figure 4A, C). For the rectangular-shaped electrodes, R_S was within 0.95 kΩ ± 100 Ω (Figure 4E), which was approximately the half of the round-shaped electrode value due to the larger electrode sites. The impedance variations from the previous chapters were also visible in the value distribution of Y_0. Over all measures, no relation between R_S and Y_0 was visible indicating that the surface porosities rather than the geometric areas were changed by the electroplating process. The angle factor alpha ranged from 0.85 to 0.94 over all electroplating processes and had no dependency to Y_0.

In the results of the pulsed current plating process, some higher derivations were visible. For these points, higher Y_0 and lower R_S values became visible indicating larger geometric surfaces from the electrode production. Y_0 of the rectangular electrodes was within 1.5 Ss$^\alpha$ to 4 Ss$^\alpha$ and therewith four times higher than Y_0 of the round-shaped electrodes with the same electroplating process. This matched the quotient of geometric surface areas and demonstrated the reliability of the electroplating process. Alpha was also in the same range as for the other plating processes with the highest variation for the highest current strength.

Platinum coatings show a good stability when using ultrasound

Peel and stimulation durability test were performed with the rectangular-shaped electrode sites (Figure 5). For the peel test, the electrode sites were coated with pulsed currents with amplitudes of 0.3 kA/m^2 (90 pulses) and 0.2 kA/m^2 (90 pulses). Prior the peel test, the electrode sites plated with 0.3 kA/m^2 displayed coating defects when ultrasound was not applied (Figure 5A). The peel test generated larger defects, and platinum particles were clearly visible on the tape used. In contrast, no defects were detected on the electrode sites coated with a current amplitude of 0.2 kA/m^2 prior the peel test (Figure 5B). However, the tape was able to remove parts of the coatings.
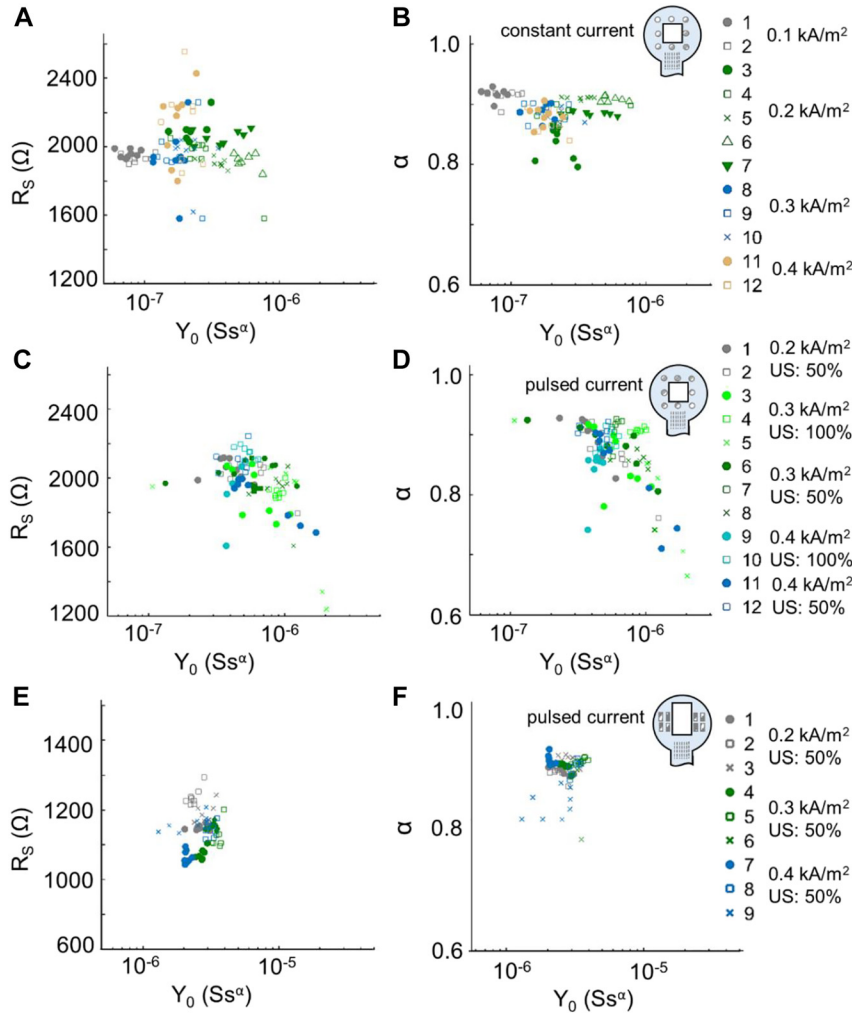
Figure 4: Electrode model parameters of the platinized electrodes.
(A, B) Solution resistor (R_S) and angle factor (α) of constant phase element (CPE) over the admittance value (Y_0) of the CPE for electroplating with constant current of the round-shaped electrodes. 1: 60 s, 2: 75 s, 3: 30 s, 4: 45 s, 5: 60 s, 6: 75 s, 7: 90 s, 8: 30 s, 9: 60 s, 10: 90 s, 11: 30 s, 12: 60 s. (C, D) R_S and α for electroplating with pulsed current of the round-shaped electrodes. 1: 60 pulses, 2: 90 pulses, 3: 60 pulses, 4: 90 pulses, 5: 120 pulses, 6: 60 pulses, 7: 90 pulses, 8: 120 pulses, 9: 60 pulses, 10: 90 pulses, 11: 60 pulses, 12: 90 pulses. (E, F) R_S and α for electroplating with pulsed current of the rectangular-shaped electrodes. 1: 60 pulses, 2: 90 pulses, 3: 120 pulses, 4: 60 pulses, 5: 90 pulses, 6: 120 pulses, 7: 60 pulses, 8: 90 pulses, 9: 120 pulses.

The electrode sites coated in the presence of ultrasound showed no defects prior and after the peel test (Figure 5C, D). Small changes in electrode placement and lighting conditions may cause the color differences in the images, which are visible at the electrode sites and at the base material. In addition, no platinum particles were visible at the tape.

The CIC was estimated for biphasic current pulses with pulse widths from 100 µs to 5 ms (Figure 5C). For a pulse width of 200 µs the values were 147–223 µC/cm^2 and for a pulse width of 500 µs 276–412 µC/cm^2. Thus, the biphasic stimulation currents for the durability test were defined to approx. 90 % of the minimum CIC currents at 530 µA (200 µs

pulse width) and 400 µA (500 µs pulse width). The results showed that for both stimulation currents the measured impedance magnitudes at 10 Hz prior and after the test were close to each other (Figure 5D).

Discussion

In order to improve the electrochemical properties of the LCP electrodes, an electroplating system for platinum electroplating was built and various electroplating parameters were tested. Owing to gas bubble formation, the use of ultrasound was essential during the electroplating process
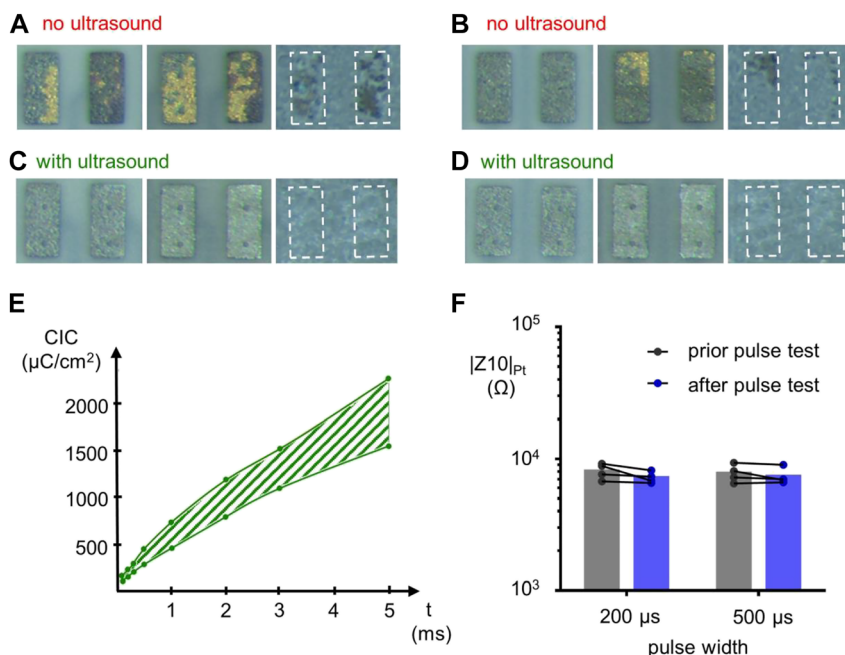
Figure 5: Electroplating stability.
(A–D) Electrode sites prior (left picture) and after (middle picture) the peel test. Right picture: Tape from the corresponding peel test. The white rectangles indicate the positions of the electrode sites during the peel test. (A) Electrode sites electroplated with 0.3 kA/m^2, 90 pulses, no ultrasound. (B) Electrode sites electroplated with 0.2 kA/m^2, 90 pulses, no ultrasound. (C) Electrode sites electroplated with 0.3 kA/m^2, 90 pulses, ultrasound 50%. (D) Electrode sites electroplated with 0.2 kA/m^2, 90 pulses, ultrasound 50%. (E) Estimation of charge injection capacity for different pulse widths. (F) Comparison of impedance magnitudes at 10 Hz prior and after a pulse test with 300.000 biphasic current pulses with amplitudes of 530 µA (pulse width: 200 µs) and 400 µA (pulse width: 500 µs).

to apply an intact platinum layer to the gold electrodes, which could be proved with optical and SEM images. In addition, a peel test showed the good adhesion of the platinum coating to the gold electrode sites when ultrasound was used. The impedance and CSC$_C$ values of the electrodes depended on site size, the material and a combined surface structure formed by a base roughness of the gold electrodes further increased by the platinum electroplating. Variations in the electroplating results per condition have most likely two reasons. The impedance values of the gold electrode sides had manufacturing tolerances and the temperature of the plating solution changed over time due to the internal ultrasonic module.

The surface structure of the platinum coatings depends on several parameters, such as the electrode overpotential, the plating current, the precursor concentration and the temperature [3]. Thus, both voltage-controlled and current-controlled electroplating processes are widely used [3–5, 12, 19–22]. The higher the electrode overpotential, the higher the deposition current and the platinum deposits are more likely to form hemispherical or unusual structures [20]. Small variations of the electrode overpotentials near to the equilibrium potential already lead to diverse crystal structures [19]. The platinum

surface can also be varied by additives in the precursor solution [21, 22] or by nanoparticles [3].

In this study, the electrode overpotential was generated by low-frequency pulsed current-controlled electroplating to optimize CIC, CSC, and impedance of the electrodes. Compared to the constant current electroplating, the low-frequency pulsed current approach displayed advantages in the impedance and the CSC of the LCP electrodes. Coatings with pulsed current densities of 0.2 kA/m^2 and 0.3 kA/m^2 show similar and stable results. Thus, we assume similar results with values between 0.2 kA/m^2 and 0.3 kA/m^2. However, it remains unclear which impact a voltage-controlled low-frequency electroplating process might have to the electrode impedance, CSC and CIC.

The best result for constant current electroplating was found at a current density of 0.2 kA/m^2 and an electroplating time of 75 s. At this time, the highest porosity for the electrodes seemed to be found resulting in the lowest electrode impedance and the highest CSC$_C$. On the one hand, the time factor was apparently decisive for whether the electrode was completely coated, which was not necessarily the case with very short times. On the other hand, the rough structures of the gold electrodes were probably smoothed by the platinum layer if the plating times were too long.

For pulse electroplating the optimization was best for a current density of 0.3 kA/m^2 and the values were similar to those of constant current electroplating (round-shaped electrode sites: |Z[f = 10 Hz]| = 32–52 kΩ as best for constant current; |Z[f = 10 Hz]| = 29–50 kΩ as best for pulsed current). For the tested parameters, however, no time dependence and a lower dependence on the current density were recognizable. This could be due to the fact that pulse electroplating produces different nucleation and plating rates within one pulse and thus inhomogeneous surfaces. The electroplating parameter with pulsed current could generated similar results for the round-shaped electrode sites to the rectangular-shaped sites (magnitude of impedance multiplied with site area for current density of 0.3 kA/m^2 and 90 current pulses: 0.54–0.9 kΩmm^2 for the round-shaped electrode sites and from 0.48 kΩmm^2 to 0.68 kAmm^2 for the rectangular-shaped electrode sites). Thus, the method showed a good robustness for the different electrode site sizes.

These LCP multichannel electrodes will be used in the murine CNS to explore the interaction of neurons and glial cells [18]. The array with round-shaped electrodes enables a higher spatial resolution in bioelectrical recording and stimulation. In contrast, the array with rectangular-shaped electrodes allows the use of higher stimulation currents and the activation of larger brain and spine regions. Therefore, this electrode was selected for the pulse test. With 300,000 pulses a total stimulation time of approx. 16.7 h at a stimulation frequency of 50 Hz is simulated. Therewith, the limited usage time in our *in vivo* animal studies [18] is covered. The results of the impedance measurements prior and after the stimulation test indicate a stable surface. However, it could not be shown whether, despite ultrasound, micro gas bubbles during electroplating may cause damage to the platinum coating and reduce binding to the gold layer. A prolonged electrical pulse test, could be performed to demonstrate the long-term stimulation stability.

Electrodes CIC depends on the material, surface porosity, electrode size, geometry, length of stimulation pulse and pulse polarity [6, 16, 17, 23–25]. Using electric current pulses with a length of 200 μs, CIC values for platinum disk electrodes of 50–100 μC/cm^2 for anodic first biphasic pulses and 100–150 μC/m^2 for cathodic first biphasic pulses were found [23]. Characterization of the Utah electrode array with platinum coating displayed a CIC value of 300 μC/cm^2 [24]. The CIC estimation of planar smooth platinum electrodes raised values of approx. 35 μC/cm^2 [17] and from 10 μC/cm^2 to 80 μC/cm^2 [16]. For microporous platinum CIC measures from 120 μC/cm^2 to 295 μC/cm^2 using a pulse length of 200 μs [16] could be

estimated. In this study, a CIC value of approx. 220 μC/cm^2 is reached. Due to the impact of the electrode geometry, a direct comparison of different plating methods must be performed at the same structure.

However, the CIC varies *in vivo* [17] and may change over application time, which may be additionally considered in a long-term evaluation. Nevertheless, the significant reduction in electrode impedance may support bioelectrical recordings with lower noise and electrical stimulation with a lower voltage across the electrode interface to drive a stimulation current. In addition, the impedance variations within an array may have less impact in multichannel recordings [9]. The CSC$_C$ is a measure of how much charge can be transferred to the electrode. An increase in CSC$_C$ for electrodes realized with the same technology also increase the stimulation current transfer capability of the electrode [16]. Although the electrode characteristics *in vivo* will be different to those determined in saline [17], the platinum coating of the electrode improves the stimulation capability of the LCP electrodes.

Conclusions

The platinum electroplating greatly improved the electrode impedance and CSC$_C$ of the gold LCP electrodes in each electroplating condition. In best cases the electroplating results are at the same level when using constant current or pulse current. However, the results of the platinum electroplating with pulsed current indicate that this method is more robust to small changes in temperature or platinum ion concentration of the electroplating solution. In addition, differences in the electroplating current (that could occur e.g., when the process is used with electrodes connected in parallel) should result in smaller variations in the electrochemical characteristics. Thus, in contrast to the constant current electroplating, the presented pulsed current electroplating had some advantages to coat the LCP electrodes.

References

1. Becker AJ. Review: animal models of acquired epilepsy: insights into mechanisms of human epileptogenesis. Neuropathol Appl Neurobiol 2018;44:112–29.
2. Bodnar CN, Roberts KN, Higgins EK, Bachstetter AD. A systematic review of closed head injury models of mild traumatic brain injury in mice and rats. J Neurotrauma 2019;36:1683–706.
3. Kloke A, von Stetten F, Zengerle R, Kerzenmacher S. Strategies for the fabrication of porous platinum electrodes. Adv Mater 2011;23: 4976–5008.
4. Ohsaka T, Isaka M, Hirano K, Ohishi T. Effect of ultrasound sonication on electroplating of iridium. Ultrason Sonochem 2008;15:283–8.
5. Boretius T, Jurzinsky T, Koehler C, Kerzenmacher S, Hillebrecht H, Stieglitz T. High-porous platinum electrodes for functional electrical stimulation. Proc IEEE Eng Med Biol Soc 2011:5404–7. https://doi.org/10.1109/IEMBS.2011.6091336.
6. Cogan SF. Neural stimulation and recording electrodes. Annu Rev Biomed Eng 2005;10:275–309.
7. Kumsa DW, Bhadra N, Hudak EM, Kelley SC, Untereker DF, Mortimer JT. Electron transfer processes occurring on platinum neural stimulating electrodes: a tutorial on the i(Ve) profile. J Neural Eng 2016;13:052001.
8. Schweigmann M, Kirchhoff F, Koch KP. Modeling and simulations in time domain of a stimulation set-up for cortical applications. Eur J Transl Myol 2016;26:116–21.
9. Englert R, Rupp F, Koch KP, Schweigmann M. Technical characterization of an 8 or 16 channel recording system to acquire spontaneous and evoked electrocorticograms of mice. Curr Dir Biomed Eng 2017;3:595–8.
10. Bagen S, Bihler E, Hauer M. Embedding of active components in LCP for implantable medical devices. In: Talk at 44th IMAPS New England symposium. US: IMAPS; 2017.
11. Boehler C, Stieglitz T, Asplund M. Nanostructured platinum grass enables superior impedance reduction for neural microelectrodes. Biomaterials 2015;67:346–53.
12. Schüttler M. Electrochemical properties of platinum electrodes in vitro: comparison of six different surface qualities. Proc IEEE Eng Med Biol Soc 2007:186–9.
13. Franks W, Schenker I, Schmitz P, Hierlemann A. Impedance characterization and modeling of electrodes for biomedical applications. IEEE Trans Biomed Eng 2005;52:1295–302.
14. Kisannagar RR, Jha P, Navalkar A, Maji SK, Gupta D. Fabrication of silver nanowire/polydimethylsiloxane dry electrodes by a vacuum filtration method for electrophysiological signal monitoring. ACS Omega 2020;5:10260–5.
15. Abu-Saude MJ, Morshed BI. Patterned vertical carbon nanotube dry electrodes for impedimetric sensing and stimulation. IEEE Sensor J 2015;15:5851–8.
16. Cisnal A, Ihmig FR, Fraile JC, Pérez-Turiel J, Muñoz-Martinez V. Application of a novel measurement setup for characterization of graphene microelectrodes and a comparative study of variables influencing charge injection limits of implantable microelectrodes. Sensors 2019;19:2725.
17. Leung RT, Shivdasani MN, Nayagam DA, Shepherd RK. In vivo and in vitro comparison of the charge injection capacity of platinum macroelectrodes. IEEE Trans Biomed Eng 2015;62:849–57.
18. Schweigmann M, Caudal LC, Stopper G, Scheller A, Koch KP, Kirchhoff F. Versatile surface electrodes for combined electrophysiology and two-photon imaging of the mouse central nervous system. Front Cell Neurosci 2021;15:720675.
19. Whalem JJ, 3rd, Weiland JD, Searson PC. Electrochemical deposition of platinum from aqueous ammonium hexachlorplatinate solution. J Electrochem Soc 2005;152:C738.
20. Guo L, Searson PC. On the influence of the nucleation overpotential on island growth in electrodeposition. Electrochim Acta 2010;55:4086–91.
21. Zátonyi A, Fedor F, Borhegyi Z, Fekete Z. In vitro an in vivo stability of black-platinum coatings on flexible, polymer microECoG arrays. J Neural Eng 2018;15:054003.
22. Stanca SE, Hänschke F, Ihring A, Zieger G, Dellith J, Kessler E, et al. Chemical and electrochemical synthesis of platinum black. Sci Rep 2017;7:1074.
23. Rose TL, Roblee LS. Electrical Stimulation with Pt electrodes. VIII. Electrochemically safe charge injection limits with 0.2 ms pulses. IEEE Trans Biomed Eng 1990;37:1118–20.
24. Negi S, Bhandari R, Rieth L, Solzbacher F. *In vitro* comparison of sputtered iridium oxide and platinum-coated neural implantable microelectrode arrays. Biomed Mater 2009;5:15007.
25. Ganji M, Tanaka A, Gilja V, Halgren E, Dayeh SA. Scaling effects on the electrochemical stimulation performance of Au, Pt, and PEDOT: PSS electrocorticography arrays. Adv Funct Mater 2017;27:1703019.